Thermochimica Acta 517 (2011) 53–62

Contents lists available at ScienceDirect

Thermochimica Acta

journal homepage: www.elsevier.com/locate/tca

Thermal and kinetic characterization of a toughened epoxy resin reinforced with carbon fibers

Carmen Branca[a], Colomba Di Blasi[b,*], Antonio Galgano[a], Eva Milella[c]

[a] Istituto di Ricerche sulla Combustione, C.N.R., P.le V. Tecchio, 80125 Napoli, Italy
[b] Dipartimento di Ingegneria Chimica, Università degli Studi di Napoli "Federico II", P.le V. Tecchio, 80125 Napoli, Italy
[c] IMAST SCarl, P.le E. Fermi, Granatello, 80055 Portici, Italy

ARTICLE INFO

Article history:
Received 7 December 2010
Received in revised form 18 January 2011
Accepted 21 January 2011
Available online 3 March 2011

Keywords:
Composite material
Oxidative decomposition
Chemical kinetics
Heat and mass transfer

ABSTRACT

The oxidation behavior of a composite material (Cycom 977-2/Priform by Cytec), based on a toughened epoxy resin reinforced with carbon fibers, is studied in the kinetic regime and a mixed thermal-diffusive regime. Thermogravimetric measurements for the composite material and the two single components support the existence of three main reaction stages. The first is the oxidative decomposition of the resin taking place at temperatures between 496 and 730 K that can be described by a reaction with an activation energy of 82 kJ/mol. The second and third reaction stages correspond to the oxidation of the resin char, that terminates at about 850 K, and at higher temperatures the oxidation of the carbon fibers, described by global kinetics with activation energies of 105 and 184 kJ/mol, respectively. The thermal history of thick samples burning in a furnace depends on the heating temperature, in nitrogen, and/or the maximum temperature, in air, caused by the reaction exothermicity. After an inert heating stage, when maximum sample heating rates are achieved, the process dynamics again show the existence of three main reaction stages whose characteristic times and temperatures are determined.

1. Introduction

Fiber reinforced polymer (FRP) composites are currently used in a wide variety of structural and thermal protection applications, including aerospace, marine, automotive, civil infrastructures, chemical processing, sporting goods and consumer products, owing to their many outstanding physical, thermal, chemical and mechanical properties [1]. These materials are usually made of glass, carbon, aramid or extended-chain polyethylene fibers with a polyester, vinyl ester, epoxy or phenolic resin matrix. In particular, FRP composites present high weight-specific stiffness which are further enhanced by sandwich elements in the form of panels [2–4]. These are commonly made of two thin and yet stiff face FRP skins which are separated by a thick lightweight and compliant core. The core structure is made from polymeric foams, end grain balsa wood or aramid (nomex) honeycomb. The faces of the panel offer a high resistance to external bending loads while the core is especially suited for resistance to external and smoothly varying shear loads. The scarce resistance to fire and the high flammability are generally the main drawbacks [5] of FRP materials, although a large thickness or the use of FRP laminates in sandwich panels with refractory core materials may improve their performances [6]. The complex interactions between chemical and physical processes during composite material combustion have been studied [7–9] but, as pointed out by Mouritz et al. [10], the research has mainly concentrated on laminates reinforced with non-combustible fibers (i.e. glass) and less research has been performed on laminates with reactive fibers and on sandwich panels.

To investigate the mechanisms that control the conversion process with the scope of improving the design of reliable and efficient thermal protection systems, in this study oxidation experiments have been made of a laminate reinforced with carbon fibers, with the commercial name of Cycom 977-2/Priform by Cytec. No information on the thermal behavior of this FRP material is available in the open literature. More specifically it is a toughened epoxy resin reinforced with carbon fibers. These are based on an innovative system consisting of a fine line of toughening fiber woven into the pre-form (instead of attempting to dissolve the toughener agent into the resin) and then processed with a proprietary resin. Typical applications include aircraft primary and secondary structure, space structure, ballistics, cryogenic tanks or any application where impact resistance and light weight are required.

The present investigation is motivated by the need to get the fundamental information on the material thermal response for evaluating its applicability as a skin in sandwich panels for the railway sector. Therefore, measurements of the burning characteristics of thermally thick samples are carried out to elucidate the role played by the heating temperature on the thermal response of

* Corresponding author. Tel.: +39 081 7682232; fax: +39 081 2391800.
E-mail address: diblasi@unina.it (C. Di Blasi).

0040-6031/$ – see front matter © 2011 Elsevier B.V. All rights reserved.
doi:10.1016/j.tca.2011.01.034

the composite material. Moreover, aimed at formulating a global oxidation mechanism, to be coupled afterwards with a transport model for the prediction of the fire behavior of sandwich panels [4], measurements of weight loss are made for the conditions typical of thermal analysis and subjected to kinetic analysis.

2. Materials and methods

The material under study is a composite material consisting of carbon fibers, specifically the Priform fibers developed by Cytec, impregnated with an epoxy resin identified with the commercial name of Cycom 977-20 again produced by Cytec. The proportion of 55.5 wt% resin and 44.5 wt% Priform fibers produces the composite material Cycom 977-2 which, before use, is subjected to a cure period of 2 h at 453 K and a post-cure period of 1 h at 473 K [11]. It is a non-porous laminate with a density of 1.47 g/cm^3 and a glass transition temperature of 485 K.

A first set of experiments has been made using a thermogravimetric system with samples preliminarily reduced to small sized particles with the scope of analyzing the thermal behavior of the material and to produce data for kinetic analysis. The experimental system has already been used for the analysis of solid fuel degradation [12–15] and only the main characteristics are discussed here. It consists of a furnace, a quartz reactor, a PID controller, a gas feeding system, an acquisition data set, and a precision balance. The furnace is a radiant chamber, which creates a uniformly heated zone, where a quartz reactor is located. The sample is exposed to thermal radiation by means of a stainless steel mesh screen, whose sides are wrapped on two stainless steel rods connected to a precision (0.1 mg) balance, which allows the weight of the sample to be continuously recorded. An air flow (nominal velocity of 0.5×10^{-2} m/s for the tests discussed in this study) establishes the proper reaction environment.

Other experiments are made to investigate the behavior of thermally thick samples of the composite material when exposed in an oxidative or inert environment under known thermal and flow conditions. The furnace integrated by a data acquisition set has also been used in previous investigations [13,16]. A schematic of the experimental system and the sample can be seen in Fig. 1. The samples (Fig. 1A) are cut in the form of parallelepids with a thickness of 0.2 cm, a length of 2 cm and a wideness of 0.5 cm. Two thermocouples are used to register the sample temperature: the first (T_i) is positioned at half thickness and a distance of 0.5 cm from the top surface, whereas the second (T_e) is positioned at the center of the top surface. Decomposition/oxidation of the sample takes place in a steel chamber (Fig. 1B) (6.5 cm internal diameter and 45 cm length), where a forced flow is distributed through a perforated plate at the bottom. A radiant furnace is used to pre-heat both the reaction chamber and the gas which is fed through a jacket (internal diameter 8.9 cm) at the reactor top. Temperature profiles along the reactor axis are measured by seven thermocouples (chromel–alumel type, 500 μm diameter), with their tips exiting from a protective steel tube, at chosen distances from the flow distributor. The lower zone (about 20 cm) is isothermal at a temperature determined by a proper selection of the furnace temperature (PID controller) indicated in the following as heating temperature, T_r.

Once the desired thermal conditions are achieved, the reactor closing cap is substituted by another one equipped with a thin steel rod acting as a support for the sample and the thermocouples used to gain information about its thermal response. In this way, the sample is suspended in the pre-heated isothermal section of the reactor with the center positioned along the axis at a distance of 3.5 cm from the flow distributor. The sample is caged by a 300 μm Nichrome wire, tied to the steel rod, to permit a direct exposition to

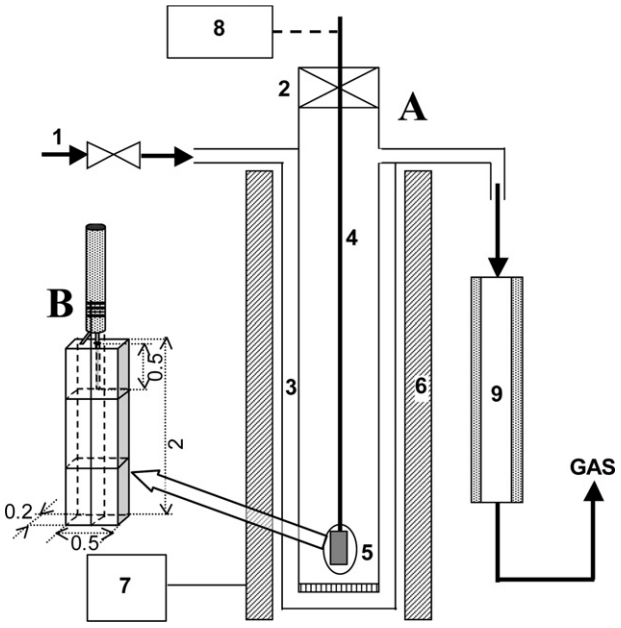

Fig. 1. Schematic of the reaction chamber (A) and the composite material sample (B, sizes in cm): (1) gas feeding point, (2) isolating valve, (3) gas heating, (4) sample holder, (5) sample and thermocouples, (6) furnace, (7) controller, (8) acquisition data set, and (9) hair pins.

thermal radiation from the chamber walls and convective heating from the forced gas flow. To minimize heat conduction rates, the thermocouples and the support are insulated by means of a ceramic tube and refractory cement. After the sample center reaches the heating temperature or higher values, the furnace is kept at the set point for 30–120 min, depending on the heating conditions, then the power is turned off. The sample is left under a forced gas flow until the temperatures lowers to 400 K, then it is collected to evaluate the characteristics of the solid residue by means of visual observation and Scanning Electron Microscope (SEM) analysis.

3. Results

In this section results are presented first of the thermogravimetric behavior of the material. Then the characteristics of the thermal response of thermally thick samples exposed in a pre-heated reaction chamber under a forced flow of air or nitrogen are discussed. Finally, a kinetic model if formulated and the related kinetic parameters are evaluated.

3.1. Thermal response for thermogravimetric conditions

Weight loss measurements are made in air for a heating rate of 5 K/min and a final temperature of 1050 K for the composite material, the epoxy resin and the carbon fibers. Experiments are made with a mass of 4 mg and particle sizes of 80 μm (resin and composite material) or about 150 μm (carbon fibers). The weight loss characteristics of the various samples can be useful to identify the main stages undergone by the composite material during oxidation. For the composite material, thermogravimetric curves are also obtained at the heating rates of 2.5, 7.5 and 10 K/min for successive kinetic analysis.

Fig. 2 reports the time profiles of the integral and differential thermogravimetric curves, for the FRP composite, the resin and the Priform carbon fibers measured at 5 K/min, and the temperature. Both the composite material and the pure resin show a zone of rapid weight loss (with a local maximum rate around 560–562 K) followed by a shoulder localized at temperatures around 695–704 K

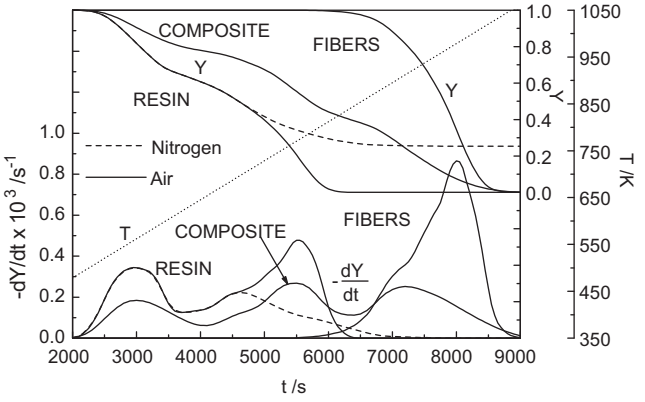

Fig. 2. Measured weight loss curves for the FRP composite and the components, resin and Priform carbon fibers, in terms of mass fraction, Y, and time derivative of the mass fraction, dY/dt (heating rate, h, 5 K/min and final temperature, T_f, 1050 K).

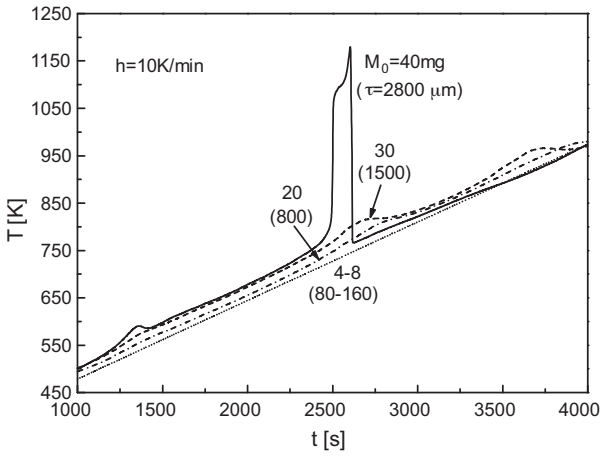

Fig. 3. Measured sample temperature for thermogravimetric tests of the composite material for various masses, M_0, and thicknesses, τ, of the sample. The assigned heat flux corresponds to a heating rate of 10 K/min for a sample of 4 mg.

(the position of the shoulder is assumed [17] to coincide with the minimum in the d^2Y/dt^2 for the region of interest). Hence, it can be postulated that a first reaction stage exists (temperatures around 496–730 K), characterized by at least two different steps of weight loss, that can be associated with the oxidative decomposition of the resin, producing volatile species and char, and the further devolatilization of char. As shown in the following, based on the results obtained for thick samples, it appears that, during the thermal/oxidative stage, the polymeric resin also undergoes melting, with the formation of a swollen porous char, for temperatures around 600 K.

The second reaction stage is the oxidation of the char produced from the oxidative degradation of the resin. Peak rates are attained around 769–772 K and the process is practically terminated around 850 K. At the higher temperatures, the last reaction stage occurs concerning the oxidation of the carbon fibers with a maximum in the rate of volatile release observed at temperatures of 912 K for the composite and 979 K for the carbon fibers. In the latter case, a well visible shoulder precedes, at shorter times (or lower temperatures), the peak zone. Presumably it is a consequence of a higher reactivity of the toughener content in the Priform fibers and/or other compounds usually present in small amounts in carbon fibers [1].

Fig. 2 also reports the weight loss characteristics for the resin in nitrogen (heating rate 5 K/min). At low temperatures (below 700 K) no appreciable difference is seen with respect to the measurement carried out in air. At higher temperatures, instead of complete oxidation, further slow devolatilization of the char occurs leading to final yields of the solid residue around 25%.

Moreover, from Fig. 2, it can be noted that the first two reaction stages in air (resin decomposition and char oxidation) take place over the same temperature range and, in particular, with the maximum rates of volatile release localized at about the same temperatures, independently from the sample being the composite or the resin. Therefore, it can be assumed that conversion is occurring under a kinetic control with negligible temperature and oxygen gradients across the small sample mass. On the contrary, the oxidation of the Priform fibers shows a peak rate significantly delayed with respect to that observed for the composite material. The larger particle size, determined by the peculiar nature of the material being processed, is responsible for a more important role of oxygen diffusion versus the intrinsic kinetics of the heterogeneous oxidation reaction. In other words, the augmented difficulty for oxygen to diffuse towards the reaction zone across thicker particles delays the oxidation process.

Additional thermogravimetric experiments have also been made in air to investigate the sample temperature variation during heating. Fig. 3 reports the sample temperature versus time as measured by a thin thermocouple in close contact with the samples as the mass and thickness are varied (from 4 to 40 mg and from 80 to 2800 μm, respectively). The assigned heat flux, preliminarily determined, corresponds to 4 mg sample heated at 10 K/min (the highest heating rate examined in this study, as heat and mass transfer limitations are more likely to become important with respect to chemical kinetics). Doubling the sample mass (and thickness) does not introduce any change in the temperature profile. It can be understood that the sequential occurrence of the three main reaction stages, discussed above, also gives rise to a sequential distribution in the reaction energetics, thus facilitating temperature control. The effects, globally exothermic, of the reaction process become evident for sample masses of 20 and 30 mg, in particular for the char and carbon fiber oxidation for temperatures above 750 and 900 K, respectively. A thermal runaway is, instead, observed with these two processes occurring simultaneously when the sample mass is 40 mg. It is worth noting that exothermic effects are also seen for sample masses of 20 mg and above, for temperatures in the range 550–600 K where decomposition of the resin takes place. It can be thought that the exothermic formation of char predominates over the endothermic formation of volatile condensable species and convective cooling [7]. From these measurements it appears that for a sample mass of 4 mg, such as used in the themrogravimetric measurements of this study, a good control of the sample temperature is achieved and the measured weight loss curves can be used for the determination of intrinsic chemical kinetics.

As the heating rate is increased, the weight loss characteristics of the FRP composite material remain qualitatively the same but the position of the peak rates are displaced at successively higher temperatures. In particular, over the range 2.5–10 K/min, the positions of the first (decomposition), second (char oxidation) and third (Priform fiber oxidation) peak rate vary in the ranges 541–583 K, 741–798 K and 902–940 K.

3.2. Thermal response of thick samples

In this section results are presented of the characteristics of the thermal response of thick samples exposed in a pre-heated reaction chamber under a forced flow of air or nitrogen. Experiments are carried out in air or nitrogen for heating temperatures comprised between 550 and 950 K and an inlet flow velocity of 0.6 cm/s. Each test has been repeated from three to five times, showing good reproducibility. The thermal history undergone by the sample is used to evaluate the heating rate, the reaction temperatures and the burning/decomposition times. The solid residues collected at

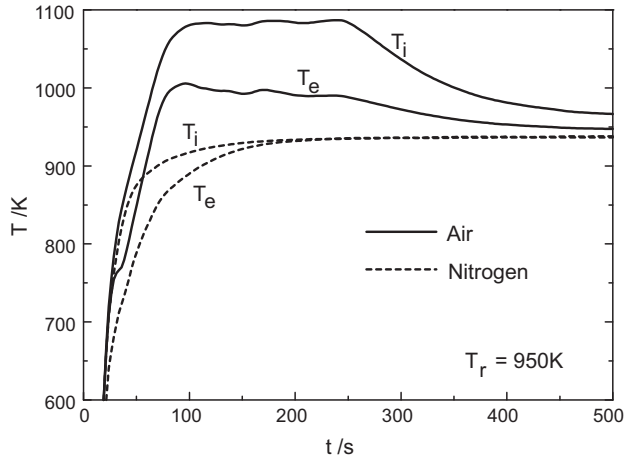

Fig. 4. Time profiles of the internal (T_i) and external temperature (T_e), as measured in air (solid lines) and nitrogen (dashed lines) for a heating temperature, T_r, of 950 K.

the conclusion of the conversion process are used to evaluate the chemico-physical changes induced in the sample structure by the thermal treatment.

An example of the heating dynamics of a thick sample of the composite material in air and nitrogen is shown in Fig. 4 for T_r = 950 K, by means of the profiles of the internal and external temperatures. The two temperature profiles are similar but T_i always shows higher values. Given the relatively small size (and mass) of the sample, the dynamics of the surface thermocouple are essentially determined by the conditions of the forced flow and the effects of the mixing between the imposed flow and the flow of decomposition/combustion products. Indeed, in the case of air flow, the extremely fuel lean mixture does not allow the proper conditions to be established for the onset of significant rates of the gas-phase oxidation reactions. The higher T_i values can be, in the first place, explained by the more important role played by radiation from the reactor walls with respect to convective heating of the sample. Moreover, in the presence of air, the walls of the hole, where the thermocouple is allocated, create a confined narrow zone where the exothermic character of the reaction of solid conversion process dominates over the characteristics of the imposed flow.

As long as the temperature remains below approximately 600 K, the profiles measured in nitrogen and air are practically coincident, indicating that there are no detectable changes in the energetic character of the decomposition reactions that are active for temperatures above the glass transition temperature of the polymeric resin (485 K). Then, in nitrogen, there is a tendency of the internal and external temperature to become coincident and to slowly tend towards the external heating temperature.

In air, heterogeneous ignition of the solid occurs with a significant activity of the oxidation reactions (smoldering) as testified by the attainment of maximum values of the internal temperature around 1100 K. In reality two zones of exothermic combustion can be seen. The first, better shown by the T_e profile, is localized between 700 and 750 K and is characterized by a very short duration and a very small exothermicity. When it is concluded, a shoulder appears indicating a slow down in the temperature rise. In accordance with the results of the thermogravimetric analysis, this zone can be attributed to the oxidation of the char produced from the oxidative decomposition of the resin component. The second wide zone with high temperature values can be attributed to the oxidation of the carbon fiber. Finally a rapid decline towards the external heating value is observed as a consequence of the complete depletion of the material.

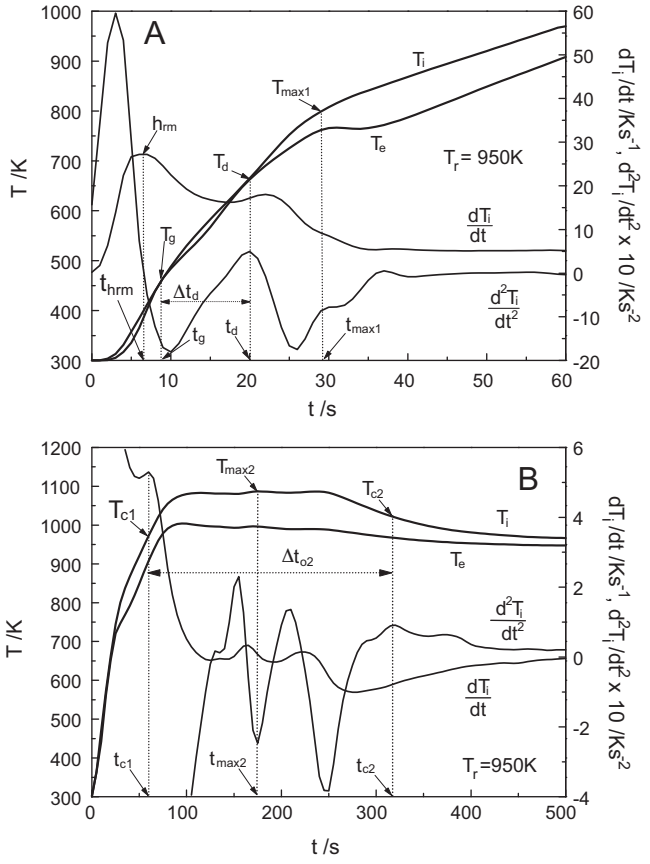

Fig. 5. Time profiles of the internal temperature, T_i, and the time derivative dT_i/dt and d^2T_i/dt^2, and the external temperature, T_e, over the interval 0–60 s (A) and 0–500 s (B) (T_r = 950 K) with the definition of process parameters: maximum heating rate, h_{rm}, and corresponding time, t_{hrm}, glass transition temperature, T_g, and corresponding time, t_g, time, t_d, and a temperature, T_d, for the conclusion of the decomposition stage, decomposition period $\Delta t_d = t_{id} - t_g$, temperature, T_{max1}, and the corresponding time, t_{max1} (oxidation of the resin char), time of the first oxidation stage, t_{c1}, and corresponding temperature, T_{c1}, time of the second oxidation stage, t_{c2}, and corresponding temperature, T_{c2}, oxidation periods, $\Delta t_{o1} = t_d - t_{c1}$ and $\Delta t_{o2} = t_{c2} - t_{c1}$, maximum temperature T_{max2}, and corresponding time, t_{max2} (the amounts of solid residues, referred to the initial mass sample for the experiments carried out in nitrogen (Y_{rd}) and air (Y_{ro}) are also introduced).

Given the weak energetic character of the thermal decomposition reactions, to get information about the characteristic times/temperatures of solid conversion, the measurements in air will be examined in detail. The thermal decomposition experiments are used to evaluate the amount of char produced from the resin decomposition and to observe the changes induced by the reactions on the material structure.

The case of a heating (air) temperature equal to 950 K is chosen to introduce the parameters that describe the thermal response of the material. Fig. 5A and B reports the profiles of the temperature T_i, and the corresponding time derivatives dT_i/dt and d^2T_i/dt^2, and the temperature T_e over the time interval 0–60 s and 0–500 s, respectively. These curves are used to define the chief process parameters, that is, the characteristic temperatures, and the duration of the stage of resin decomposition, char oxidation and carbon fiber oxidation. It appears (Fig. 5A) that, after a very rapid temperature rise, associated with inert material heating, the heating rate is reduced most likely as a consequence of the endothermicity of the decomposition reactions and the cooling effect associated with the release of hot volatile products. A time, t_{hrm}, with the corresponding maximum heating rate, h_{rm} and a time, t_g, when the glass transition temperature, T_g, is achieved can be easily read from Fig. 5A. As anticipated, the thermogravimetric curves indicate temperatures

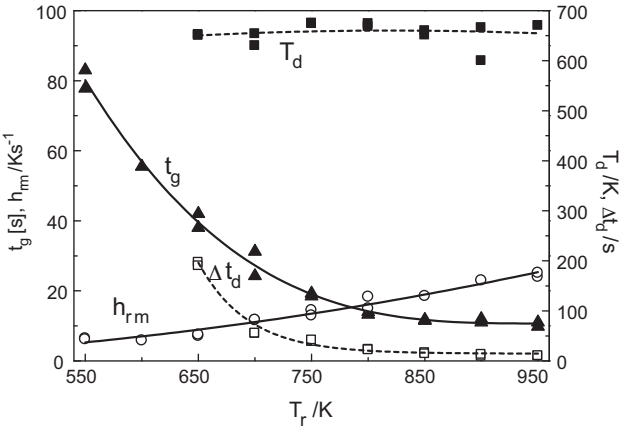

Fig. 6. Maximum heating rate, h_{rm}, characteristic times (t_g, Δt_d), and decomposition temperature, T_d, versus the heating temperature, T_r (definitions as in Fig. 5).

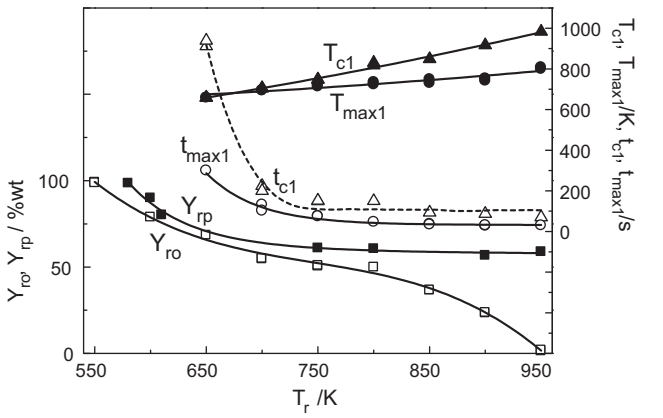

Fig. 7. Maximum temperature, T_{max1}, and corresponding time, t_{max1}, and conversion time, t_{c1}, and corresponding temperature, T_{c1}, and solid residues (Y_{rd}, Y_{ro}) collected at the conclusion of the experiments versus the heating temperature, T_r (definitions as in Fig. 5).

for the beginning of the decomposition process around 486–490 K, which are barely higher then the glass transition temperature. Thus, for simplicity, in the analysis of the dynamics of thick sample conversion, the beginning of the decomposition process is assumed to coincide with the glass transition temperature. Moreover, a time, t_d, and a temperature, T_d, are also defined corresponding to the conclusion of the decomposition stage, assumed to coincide with the second local maximum in d^2T_i/dt^2 (that is, when dT_i/dt presents an inflection point, testifying the conclusion of an endothermic process). Thus, the decomposition period is $\Delta t_d = t_d - t_g$. A temperature, T_{max1}, and the corresponding time, t_{max1}, can also be identified corresponding to a first well defined maximum on the T_e profile, that can be associated with the maximum activity of the oxidation reaction of the char made available from the decomposition reactions. The simultaneous onset of the oxidation reaction of the carbon fibers does not permit a univocal determination of this point from the T_i curve, whereas a better resolution in the separation between the oxidation reactions of the resin char and the carbon fibers is shown by the external temperature which, in this way, permits an easier definition of the second reaction stage.

Fig. 5B shows the conclusion of the first oxidation stage and the attainment of very high temperatures, associated with the oxidation of carbon fibers. More precisely, the conclusion of the first oxidation stage, t_{c1}, and the corresponding temperature, T_{c1}, are assumed to coincide with the third local maximum in dT_i/dt (detected at times longer than t_{max1}), that represents the beginning of the fiber oxidation stage. The conclusion of this second oxidation stage, t_{c2}, and corresponding temperature, T_{c2}, are assumed to coincide with the last local maximum in d^2T_i/dt^2. Hence, the first oxidation period is $\Delta t_{o1} = t_{c1} - t_d$ and the second oxidation period is $\Delta t_{o2} = t_{c2} - t_{c1}$. Fig. 4B also shows the maximum temperature, T_{max2}, and the corresponding time, t_{max2}, which represent the conditions of maximum activity of the oxidation reactions of carbon fibers. Finally, the amounts of solid residues are evaluated with reference to the initial mass sample for the experiments carried out in nitrogen (Y_{rd}) and air (Y_{ro}).

The parameters, introduced through Fig. 5A and B, are obtained from various measurements and reported versus the heating temperature, T_r, in Figs. 6–8 (results for several conditions are missing because not all the parameters can be defined over the entire range of heating temperatures examined). Examples of the measured temperatures versus time profiles for various T_r are shown in Fig. 9. In all cases, the maximum heating rate is achieved at very short times, before the attainment of the glass transition temperature. It becomes successively higher and shows a linear dependence on T_r with values roughly comprised between 6.5 and 25 K/s. The time needed to achieve the glass transition temperature is also rather short and decreases as T_r is increased (from about 80 to 10 s). It is indicative of the duration of the initial (inert) heating stage. Then, reactions begin that concerns oxidative decomposition of the resin and oxidation of the char and carbon fibers.

Based on the characteristic temperatures introduced above and in agreement with the results of thermogravimetric analysis, it appears that decomposition takes place for temperatures approximately between the glass transition temperature, 485 K, and the maximum T_d value, 670 K. In reality, the latter temperature varies in a narrow range, about 650–670 K (the definition of this parameter for this reaction stage is not possible for heating temperature below 650 K), indicating that oxidative decomposition is a low temperature process. The duration of the oxidative decomposition process (200–20 s) is longer that that of the inert heating stages for heating temperatures below 800 K. Then both stages become very short and take about 15–10 s each. For the relatively low temperatures characterizing the decomposition of the resin component and the relatively small sample size, it is likely that the process characteristics are mainly determined by the rates of external heat transfer.

To understand the characteristics of the oxidation process, it is useful to observe the changes undergone by the composite material during the conversion process. For the experiments carried out in nitrogen, significant conversion is observed only for heating temperatures above 600 K. For T_r = 610 K the char yield is about 35.5%

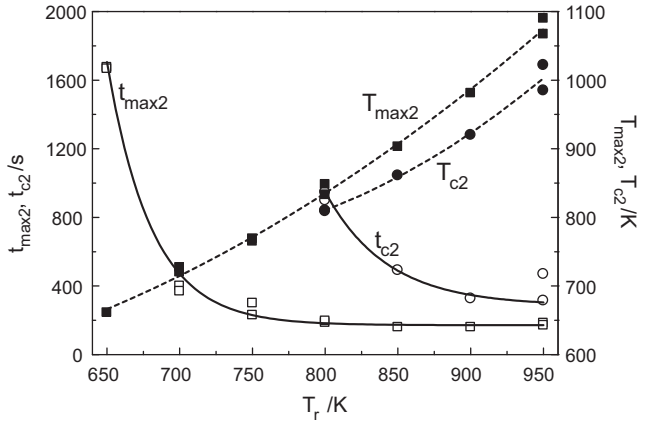

Fig. 8. Maximum temperature, T_{max2}, and corresponding time, t_{max2}, and conversion time, t_{c2}, and corresponding temperature, T_{c2}, versus the heating temperature, T_r (definitions as in Fig. 5).

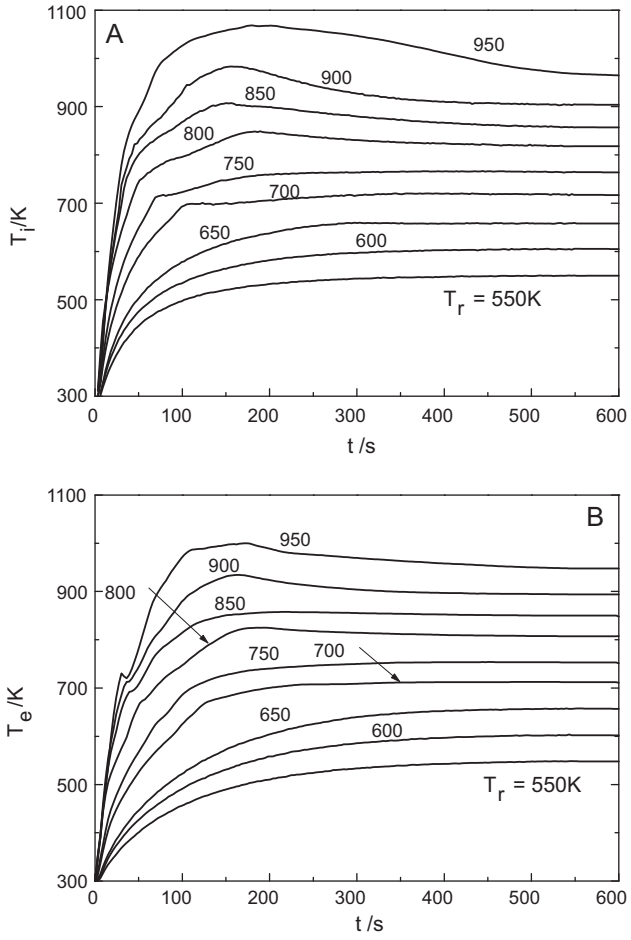

Fig. 9. Time profiles of the internal temperature, T_i, (A) and external temperature, T_e, (B) as measured for several heating temperatures, T_r.

(the total residue, also including the carbon fiber, amounts to 80%). Then, when the temperature is made to increase up to 950 K the char yield decrease to about 25% (total residue yield of 58%). Hence sample devolatilization in nitrogen is successively more favored with respect to char formation as the temperature is increased.

At low heating temperatures (below 650 K), the total solid residues collected from the experiments in air are slightly lower than those obtained in inert environment, plausibly as a consequence of a small activity of the oxidation reactions. Then, at higher temperatures, conversion becomes successively higher, as a consequence of the oxidation reactions, until no residue is detected (T_r = 950 K).

Visual observation of the residue obtained in nitrogen reveals the formation of solidified bubbles at the surface indicating that the material undergoes a molten phase while degrading. The physicochemical changes undergone by the resin and the composite when exposed in a high temperature reaction chamber can be seen through Figs. 10A, B and 11A, B, which report photographs of the thick samples before and after heating in nitrogen. The experiments foresee a preheating period of the furnace up to 610 K and an exposure of the samples at this temperature for 60 min. Then the temperature is slowly (heating rate 4 K/min) increase to 750 K. After a further retention time of 35 min, the power is turned off and the sample is left under a continuous nitrogen flow until the temperature lowers to 400 K. Then samples are collected and photographs are produced. Low temperatures and slow heating rates are used to avoid the possible transport of the molten phase away from the sample by the volatile products and the external forced flow. It can be seen that the original sample shape is lost (especially for the resin) following melting and formation of a swollen char that is quite fragile. Owing to the anisotropic properties of the resin (and the cuts for producing the samples) and/or the presence of carbon fibers, the molten phase mainly flow across the sample thickness giving rise to the formation of assemblies of small bubbles that then solidify into a highly porous char.

SEM pictures of residues from the low-temperature experiments confirm the formation of a molten phase. Examples of SEM pictures are shown in Fig. 12 of the virgin composite material (A and B), and residues collected from the oxidation experiments for a heating temperature of 600 K (C and D), 650 K (E and F) and 800 K (G and H). The unreacted material (thickness) shows that the carbon fibers are embedded by the epoxy resin. Internal sections of the residues collected from the experiments carried out in air at 600 K indicate that the amount of char still cover a large part of the carbon fibers and that the polymeric resin undergoes a molten phase while degrading. The change in the state is more evident as the heating temperature is increased from 600 to 650 K. At higher temperatures, complete conversion of the resin char takes places so that the residue only consists of carbon fibers. These show a diameter of 7 μm with the external surface crossed by parallel furrows.

The first oxidation stage occurs with maximum temperatures that are always much lower than the heating temperatures. Sample residues collected at the conclusion of the experiment show that, for heating temperatures below 650 K, the resin char is not significantly oxidized. In reality the rate of the oxidation reaction, based on the results of the thermogravimetric analysis, attains significant values only for temperatures above 730 K when the percentage of the resin char are significantly reduced. Furthermore, they are probably not completely oxidized owing to the carbon fibers that hinder oxygen diffusion towards the most internal regions of the sample. Melting might also be a cause for a partial sample loss, thus reducing the actual char mass available for the oxidation reactions.

A combination of these factors is responsible for the relatively small effects of the exothermicity of the oxidation reactions of char on the temperature profiles (T_{max1} between 660 K (T_r = 650 K) and 800 K (T_r = 950 K)). On the other hand, for heating temperatures above 800 K, oxidation of the carbon fibers attain significant rates which are partly responsible for the higher T_{c1} values. The interval Δt_{o1} approximately varies between 900 and 60 s. Given the thick samples, it can be postulated that this conversion stage is dominated by heat and mass (oxygen) transfer more than by chemical oxidation kinetics.

The oxidation of the carbon fibers is the stage responsible for the high temperatures attained by the samples with maximum variations with respect the heating temperature from about 10 K (T_r = 650 K) to 150 K (T_r = 950 K), although for low heating temperatures the process is barely active and the conclusion of the process cannot be determined. Moreover, the position of the maximum temperature is observed at successively shorter times (1670–190 s) as T_r is increased up to 800 K. Then it becomes approximately constant, indicating that the process is driven by the heat released by the reaction and not by the imposed heating conditions. Again, supported by the high exothermicity of the reaction, pure kinetic limitations are not likely to exist. Instead, also taking into account the heterogeneous nature of the oxidation process, diffusion of oxygen towards the reaction zone of the sample is plausibly the controlling mechanism.

3.3. Kinetic analysis

Similar to the approach used for both natural and synthetic polymers [16–20], the two processes of oxidative devolatilization of the FRP composite and heterogeneous oxidation of the solid residue

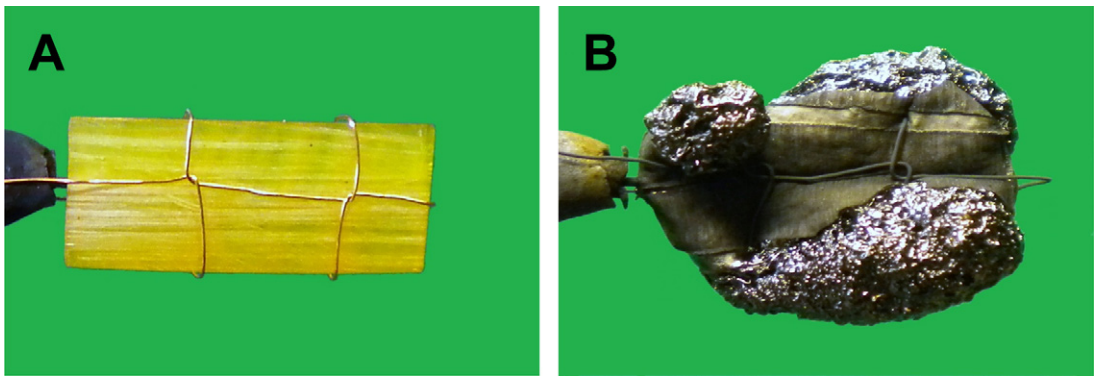

Fig. 10. Photograph of a thick (0.2 cm) resin sample before (A) and after exposure (B) to heating in nitrogen (60 min at 610 K, heating at 4 K/min up to 750 K, 35 min at 750 K).

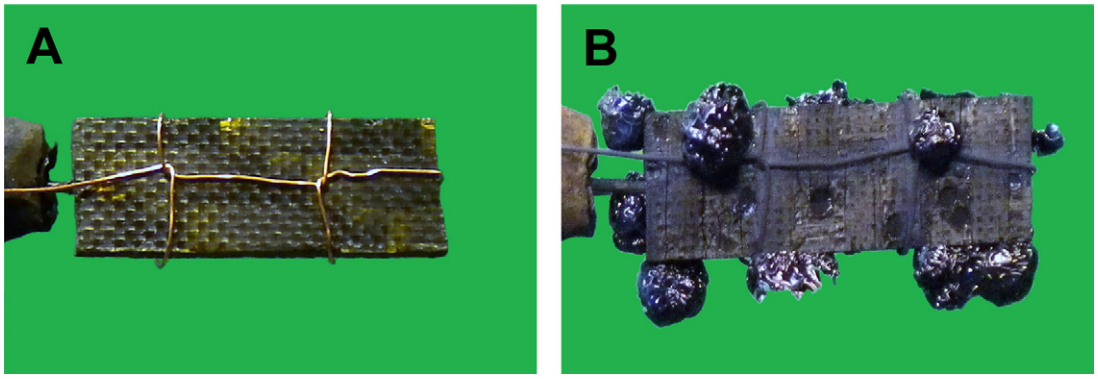

Fig. 11. Photograph of a thick (0.2 cm) composite sample before (A) and after exposure (B) to heating in nitrogen (60 min at 610 K, heating at 4 K/min up to 750 K, 35 min at 750 K).

(resin char and carbon fibers) are described by a set of parallel reactions for the lumped volatile components. Then, the overall mass loss rate is a linear combination of the single component rates. The parallel reaction mechanism is general as it can properly take into account the various steps by an appropriate set of parameter values and, at the same time, can describe well their possible overlap. Usually the number of reactions is a process parameter that needs to be estimated. However, the examination of the thermogravimetric curves suggests that, for an accurate description of the integral and differential data for the FRP composite, *S*, three reactions are required:

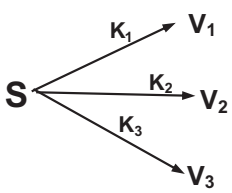

resin decomposition (a1)

char oxidation (a2)

carbon fibers oxidation (a3)

Reaction (a1) is assumed to describe the formation of volatiles from the oxidative devolatilization of the resin, reaction (a2) the oxidation of the resin char while reaction (a3) deals with the oxidation of the carbon fibers. The reactions rates present the usual Arrhenius dependence (A_i are the pre-exponential factors and E_i are the activation energies) on the temperature and a linear (decomposition) or a power law (oxidation, exponent n) dependence on the lumped volatile solid mass fractions. The latter treatment takes into account the evolution of the pore surface area during conversion [20].

The sample temperature is a known function of time, so the mathematical model consists of three ordinary differential equations for the lumped volatile mass fractions, Y_i, where the parameters ν_i, indicated in the following as stoichiometric coefficients, are the initial mass fractions of the lumped classes of volatiles generated that should be estimated:

$$\frac{\partial Y_i}{\partial t} = -A_i \exp\left(\frac{-E_i}{RT}\right) Y_i^{n_i}, \quad Y_i(0) = \nu_i, \quad i = 1, \ldots, 3 \qquad \text{(b1–b3)}$$

Other parameters to be estimated are the activation energies ($E_1 - E_3$), the pre-exponential factors ($A_1 - A_3$) and the reaction order (n_2,n_3). The task is accomplished through the numerical solution (implicit Euler method) of the mass conservation equations and the application of a direct method for the minimization of the objective function, which considers both integral (TG) and differential (DTG) data, following the method already described [13]. Deviations between the predicted and measured curves are expressed as in Ref. [13]. The simultaneous use of experimental data measured for several heating rates (2.5, 5, 7.5 and 10 K/min) avoids possible compensation effects in the kinetic parameters. The procedure of parameter estimation has been implemented using guessed values as initial estimates for the various parameters.

Fig. 13A and B reports the integral (TG) and differential (DTG) curves versus the temperature for the FRP composite as measured (symbols) and predicted by the kinetic model (lines). Details about the components are shown in Fig. 14A and B for the case of a heating rate of 5 K/min. Estimated kinetic parameters are listed in Table 1. It has been found that the estimated parameters are independent of the heating rates. Deviations between the measured and predicted curves are listed in Table 2. As testified by these values and curves shown in Figs. 13 and 14 the agreement between measurements and predictions is good. The first reaction step concerns the release of 20% of volatile matter and is described by an activation energy of 82 kJ/mol. The activation energy of the reaction for the resin char oxidation step

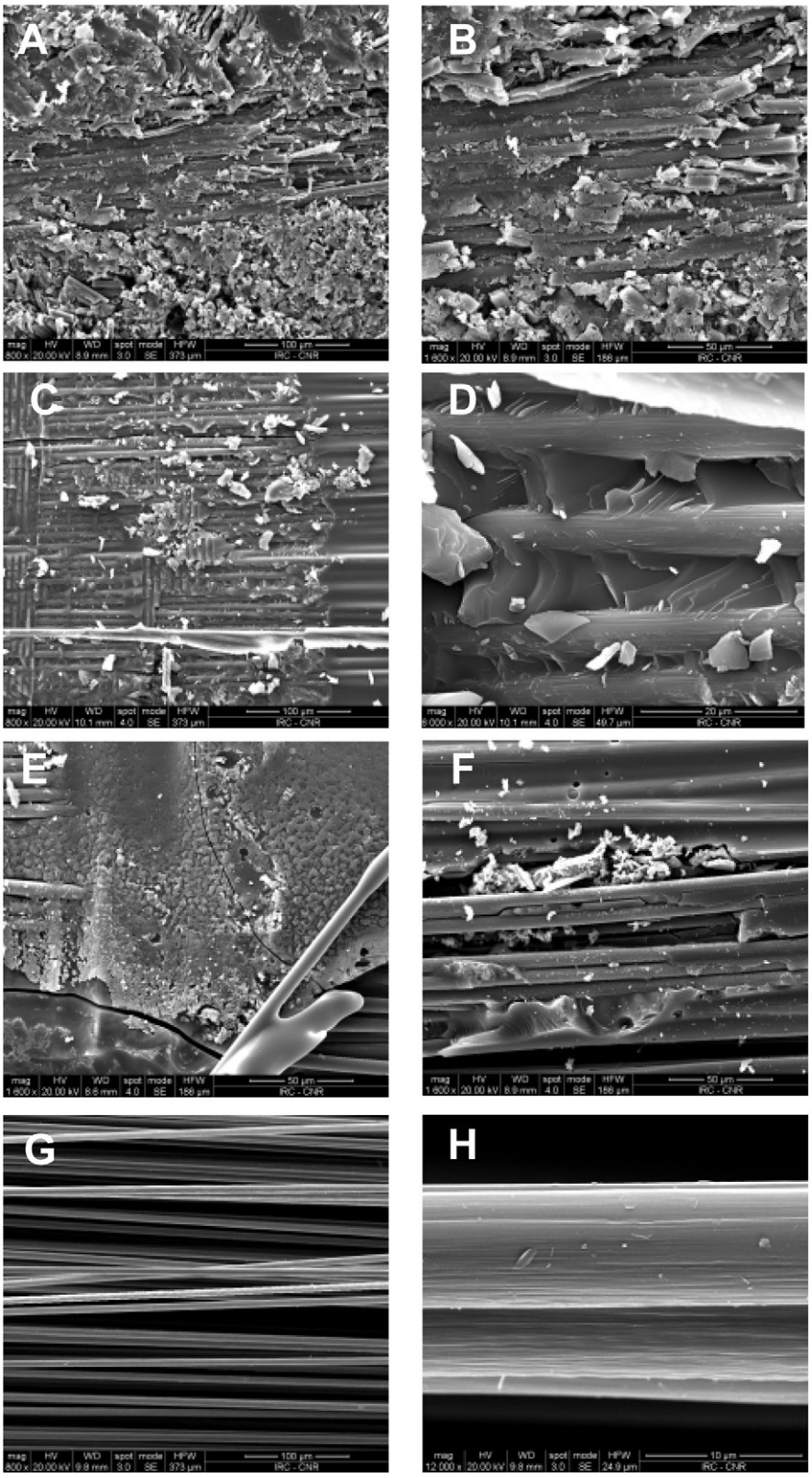

Fig. 12. SEM pictures of the composite material and composite material residues (A and B: views of the unreacted sample and the residues from oxidation experiments for a heating temperature of 600 K (C and D), 650 K (E and F) and 800 K (G and H)).

is 104.6 kJ/mol, a value relatively low testifying the high oxygen reactivity of this residue. The amount of volatile products formed from the reaction of char oxidation (35.5%) is the complement in the fraction of the resin constituting the FRP material. Consequently the reaction of carbon fiber oxidation accounts for the evolution of 44.5% volatile matter. It is described by a high activation energy, 184 kJ/mol, typical of graphite and other carbonaceous materials [20].

Table 1
Kinetic parameters (A_i, E_i, n_i) for the reaction mechanism of the composite material and the two components.

Parameter	Composite (air)	Resin (air)	Resin (nitrogen)	Carbon fibers (air)
E_1 (kJ/mol)	82.0	82.0	82.0	–
A_1 (s^{-1})	1.4×10^5	1.4×10^5	1.4×10^5	–
n_1	1.25	1.25	1.25	–
ν_1	0.20	0.36	0.36	–
E_2 (kJ/mol)	104.6	104.6	90.5	–
A_2 (s^{-1})	3.2×10^4	3.2×10^4	1.1×10^4	–
n_2	1.07	1.07	1.60	–
ν_2	0.355	0.64	0.39	–
E_3 (kJ/mol)	184.0	–	–	184.0
A_3 (s^{-1})	1.2×10^8	–	–	1.4×10^7
n_3	1.75	–	–	0.91
ν_3	0.445	–	–	1

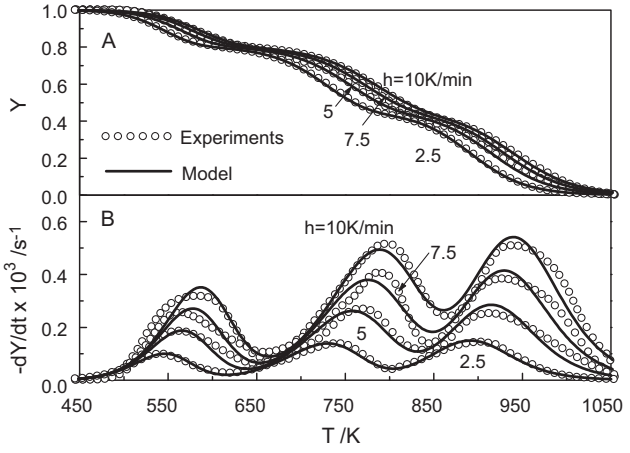

Fig. 13. Predictions (lines) and measurements (symbols) of the total mass fractions (A) and weight loss rates (B) for the FRP composite at four different heating rates, h, versus temperature (kinetic parameters listed in Table 1).

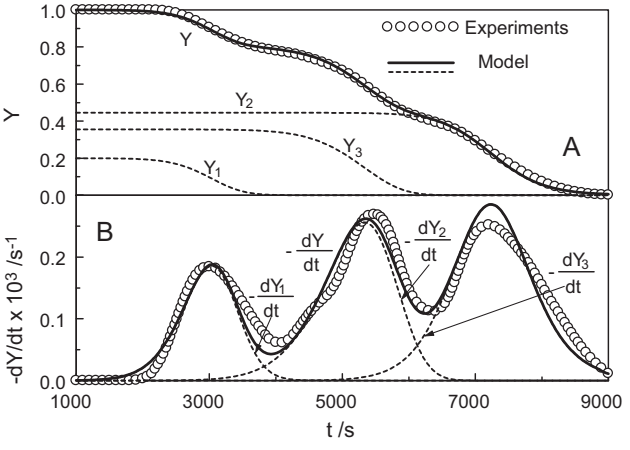

Fig. 14. Predictions (lines) and measurements (symbols) of the total and components mass fractions (A) and weight loss rates (B) for the FRP composite for a heating rate, h, of 5 K/min (kinetic parameters listed in Table 1).

Table 2
Deviations between measurements and predictions for the integral (TG) and differential (DTG) weight loss characteristics (kinetic parameters listed in Table 1).

Material	h (K/min)	dev_{TG} (%)	dev_{DTG} (%)
Resin (air)	5	1.341	7.502
Resin (nitrogen)	5	1.216	7.313
Carbon fibers (air)	5	0.457	2.234
Composite (air)	2.5	0.354	3.884
Composite (air)	5	0.855	6.886
Composite (air)	7.5	0.758	6.732
Composite (air)	10	0.631	5.015

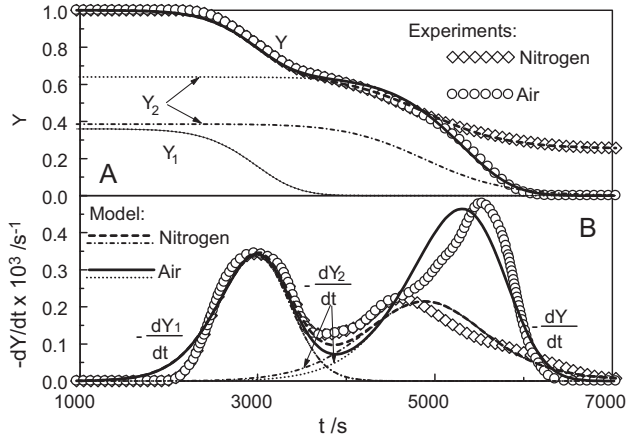

Fig. 15. Predictions (lines) and measurements (symbols) of the total and components weight loss rates for the resin mass fractions (A) and weight loss rates (B) for a heating rate, h, of 5 K/min (kinetic parameters listed in Table 1).

An attempt has also been made to describe the thermogravimetric curves obtained at 5 K/min for the resin and the Priform fibers using the same kinetic parameters already determined for the FRP composite. Exactly the same parameters are obtained for the resin conversion in air, apart from the obvious differences in the amounts of volatile matter released. The same parameters are also estimated for the decomposition step in nitrogen. Moreover, the sequential slow devolatilization of char requires a further reaction step with an activation energy of 90.5 kJ/mol and an exponent for the power law dependence on the solid mass fraction of 1.6. The same activa-

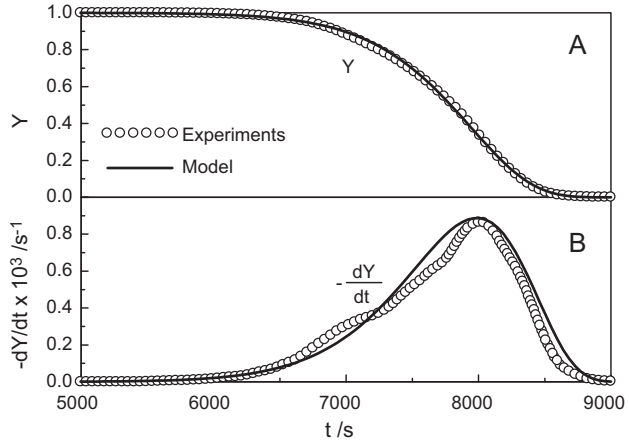

Fig. 16. Predictions (lines) and measurements (symbols) of the mass fraction (A) and weight loss rates (B) for the Priform carbon fibers for a heating rate, h, of 5 K/min (kinetic parameters listed in Table 1).

tion energy is also obtained for the oxidation of the Priform fibers with small variations on the other two parameters attributable to possible experimental errors, interactions among components and the presence of mass transfer limitations for the experiment. The complete set of kinetic parameters for the components is also listed in Table 1. A comparison between predictions and measurements, including component details, reported in Figs. 15 and 16 for the differential curves, shows an acceptable agreement.

4. Conclusions

The oxidation behavior is studied of a toughened epoxy resin reinforced with carbon fibers (Cycom 977-2/Priform by Cytec) with the scope of evaluating its thermal performances as a first step in the evaluation of its possible application as a skin in sandwich panels. Moreover, the analysis also considers the formulation of a global oxidation mechanism to be successively incorporated in a transport model for the simulation of the panel dynamics. Two set of experiments are carried out with a small sample mass in air with a thermogravimetric system for heating rates between 2.5 and 10 K/min and a final temperature of 1050 K and with thick samples in a reaction chamber under a continuous air or nitrogen flow (0.6 cm/s) at temperatures between 550 and 950 K.

Thermo-gravimetric measurements, carried out for the composite material and its two components (resin and Priform carbon fibers), are used to identify the main reaction steps taking place during the oxidation process. An oxidation mechanism is proposed consisting of one reaction for the oxidative decomposition of the resin (activation energy of 82 kJ/mol), one reaction for the oxidation of the resin char (activation energy of 104.5 kJ/mol) and one reaction for the oxidation of the carbon fibers (activation energy of 184 kJ/mol). In addition to chemical transformations, the polymeric resin also undergoes melting for temperatures around 600 K.

The analysis carried out for thermally thick samples shows that the conversion degree of the composite depends on the heating temperature (nitrogen) and/or the maximum temperature (air) achieved by the sample as a consequence of the exothermicity of the reactions for the oxidation of the resin char and the carbon fibers. Again, three main dynamic stages are observed in accordance with the proposed oxidation mechanism, integrated by additional information on the thermal performances of the material. Maximum heating rates, observed well before the onset of the chemical reactions, reach values of 6.5–25 K/s. The resin undergoes melting with decomposition completed over a rather narrow temperature range (650–670 K). The corresponding times vary from 200 to 20 s for heating temperatures between 650 and 800 K and then are reduced to 15–10 s. Oxidation of the relatively small amounts of resin char exhibits small maximum temperatures, also owing to the shield action exerted by carbon fibers towards oxygen diffusion, thus hindering complete oxidation, and probably the partial loss of the sample following melting. On the contrary, the exothermic effects of carbon fiber oxidation are significant especially for heating temperatures above 800 K when the local temperature drop reaches 50–150 K. Moreover, as the heating temperature is increased up to 800 K the times needed to attain the maximum become successively shorter (1670–190 s) but then they become constant indicating a processes controlled by the internal heat transfer rate and the oxygen diffusion rate driving the oxidation reactions.

Acknowledgments

This work is part of the activities carried out in the framework of the project PIROS “Progettazione integrata di componenti multifunzionali per applicazioni in sistemi del settore ferrotranviario e dei vettori di medie dimensioni, associata alla realizzazione di speciali facilities per prove e qualificazioni di materiali in condizioni di fiamma”, coordinated by IMAST and funded by the Italian Ministry of Instruction, University and Research (MIUR), the partial support of which is gratefully acknowledged. The authors also thank Dr. Mauro Zarrelli (IMCB-CNR, Portici, IT) for providing the samples used for thermogravimetric analysis.

References

[1] A.P. Mouritz, A.G. Gibson, Fire Properties of Polymer Composite Material, Springer, Dordrecht, The Netherlands, 2006.
[2] C.A. Ulven, U.K. Vaidya, Composites A 37 (2006) 997–1004.
[3] C.A Ulven, U.K. Vaidya, Composites B 39 (2008) 92–107.
[4] A. Galgano, C. Di Blasi, C. Branca, E. Milella, Polym. Degrad. Stab. 94 (2009) 1267–1280.
[5] A.P. Mouritz, Z. Mathys, C.P. Gardiner, Composites B 35 (2004) 467–474.
[6] A.G Gibson, Y.S. Wu, H.W. Chandler, J.A.D. Wilcox, P. Bettes, Revue de l'Institut Francais du Petrole 50 (1995) 69–74.
[7] C. Di Blasi, Polym. Int. 49 (2000) 1133–1146.
[8] J. Staggs, Mathematical modeling, in: A.R. Horrocks, D Price (Eds.), Fire Retardant Materials, Woodhead Publishing Limited, Cambridge, 2001, pp. 398–420.
[9] J. Staggs, Polym. Degrad. Stab. 82 (2003) 297–307.
[10] A.P. Mouritz, S. Feih, E. Kandare, Z. Mathys, A.G. Gibson, P.E. Des Jardin, S.W. Case, B.Y. Lattimer, Composites A 40 (2009) 1800–1814.
[11] M. Zarrelli, personal communication, 2009.
[12] C. Di Blasi, C. Branca, Ind. Eng. Chem. Res. 40 (2001) 5547–5556.
[13] C. Branca, C. Di Blasi, H. Horacek, Ind. Eng. Chem. Res. 41 (2002) 2104–2114.
[14] C. Branca, C. Di Blasi, Thermochim. Acta 456 (2007) 120–127.
[15] C. Branca, C. Di Blasi, Fire Safety J. 43 (2008) 317–324.
[16] C. Di Blasi, C. Branca, A. Galgano, R. Moricone, E. Milella, Polym. Degrad. Stab. 94 (2009) 1962–1971.
[17] M.G. Gronli, G. Varhegyi, C. Di Blasi, Ind. Eng. Chem. Res. 41 (2002) 4201–4208.
[18] G. Varhegyi, M.J. Antal, E. Jakab, P. Szabo, J. Anal. Appl. Pyrolysis 42 (1996) 73–87.
[19] C. Di Blasi, Prog. Energy Combust. Sci. 34 (2008) 47–90.
[20] C. Di Blasi, Prog. Energy Combust. Sci. 35 (2009) 121–140.